ACS central science

Research Article

Cite This: ACS Cent. Sci. XXXX, XXX, XXX−XXX

# End-On Bound Iridium Dinuclear Heterogeneous Catalysts on $WO_3$ for Solar Water Oxidation

Yanyan Zhao,[†,#] Xingxu Yan,[‡,#] Ke R. Yang,[§,#] Sufeng Cao,[∥] Qi Dong,[†] James E. Thorne,[†] Kelly L. Materna,[§] Shasha Zhu,[†] Xiaoqing Pan,[‡,⊥] Maria Flytzani-Stephanopoulos,[∥] Gary W. Brudvig,[§] Victor S. Batista,[§] and Dunwei Wang*[,†]

[†]Department of Chemistry, Merkert Chemistry Center, Boston College, Chestnut Hill, Massachusetts 02467, United States

[‡]Department of Chemical Engineering and Materials Science and [⊥]Department of Physics and Astronomy, University of California - Irvine, Irvine, California 92697, United States

[§]Yale Energy Sciences Institute and Department of Chemistry, Yale University, New Haven, Connecticut 06520, United States

[∥]Department of Chemical and Biological Engineering, Tufts University, Medford, Massachusetts 02155, United States

Supporting Information

**ABSTRACT:** Heterogeneous catalysts with atomically defined active centers hold great promise for high-performance applications. Among them, catalysts featuring active moieties with more than one metal atom are important for chemical reactions that require synergistic effects but are rarer than single atom catalysts (SACs). The difficulty in synthesizing such catalysts has been a key challenge. Recent progress in preparing dinuclear heterogeneous catalysts (DHCs) from homogeneous molecular precursors has provided an effective route to address this challenge. Nevertheless, only side-on bound DHCs, where both metal atoms are affixed to the supporting substrate, have been reported. The competing end-on binding mode, where only one metal atom is attached to the substrate and the other metal atom is dangling, has been missing. Here, we report the first observation that end-on binding is indeed possible for Ir DHCs supported on $WO_3$. Unambiguous evidence supporting the binding mode was obtained by *in situ* diffuse reflectance infrared Fourier transform spectroscopy and high-angle annular dark-field scanning transmission electron microscopy. Density functional theory calculations provide additional support for the binding mode, as well as insights into how end-on bound DHCs may be beneficial for solar water oxidation reactions. The results have important implications for future studies of highly effective heterogeneous catalysts for complex chemical reactions.

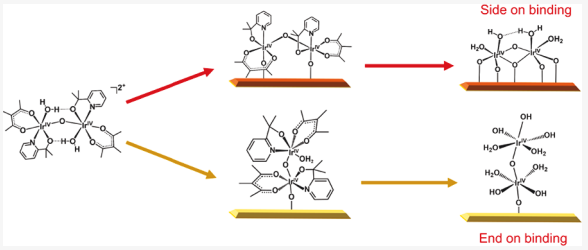


## INTRODUCTION

Research on catalysis has been traditionally divided into subfields of molecular catalysis and heterogeneous catalysis, depending on the nature of the catalysts that are being studied. Such a division has played a positive role in the development of the respective subfields because there are indeed significant differences in the methodologies best suited for the studies of these different systems. The understanding of catalysis, however, has advanced to a point where we see a clear need for convergence, as manifested by a rapidly growing body of literature aimed at advancing both molecular and heterogeneous catalysts. On the one hand, the rich knowledge of molecular catalysis makes it possible to tailor-design and fine-tune catalyst activities for ever-better performance as measured by metrics such as turnover frequencies (TOFs).[1] On the other hand, the outstanding stability of heterogeneous catalysts renders them a desired form for practical applications as measured by metrics such as high overall turnover numbers (TONs).[2] Together, a heterogeneous catalyst that features active moieties with molecular level understanding and control is the most coveted for both activity and longevity.[3] More importantly, such a catalyst would be far more versatile for a wide range of chemical transformations. Indeed, within the context of solar fuel synthesis, significant efforts have been recently undertaken toward the direction of heterogenizing molecular catalysts. For instance, Meyer et al. have pioneered this area by anchoring Ru mononuclear and dinuclear water oxidation catalysts (WOCs) onto metal oxides.[4−6] Similar approaches have been demonstrated by Sun et al. on Ru- and Co-based molecular WOCs.[7,8] To this end, some of us (Brudvig and Batista) have shown that Ir-based heterogenized molecular catalysts are more active than the amorphous oxide derivatives, highlighting the importance of maintaining the molecular structure for the reactivity.[9,10] Similarly, Tilley and Bell et al. have immobilized Co- and Mn-based molecular catalysts onto $SiO_2$.[11,12] Li et al. have also demonstrated both photoelectrochemical (PEC) and photocatalytic water oxidation on anchored Co molecular catalysts.[13,14] For the reduction reactions, Reisner et al. have coupled $TiO_2$ with Ni- and Co-

Received: May 26, 2018

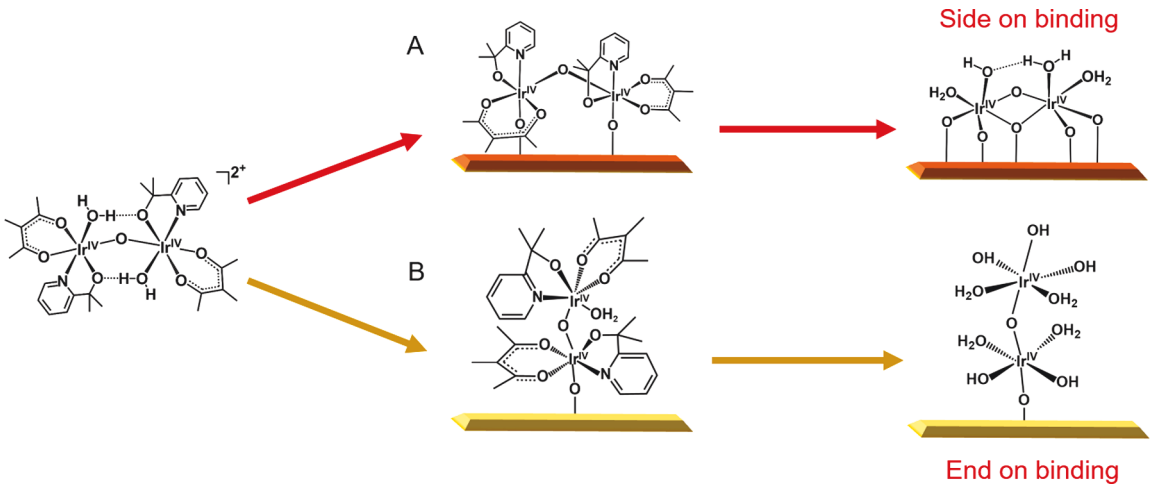


**Figure 1.** Schematics of our synthesis strategy for side-on and end-on bound DHCs. Starting from molecular dinuclear precursors, the catalyst is first adsorbed onto a substrate, and then the organic ligands are removed by photochemical treatments. The binding mode is defined by the structure of the substrate. When dual binding sites with the suitable density and distance are available (such as on $Fe_2O_3$, panel A), a side-on mode is preferred. Otherwise, the end-on mode is preferred (such as on $WO_3$, panel B).

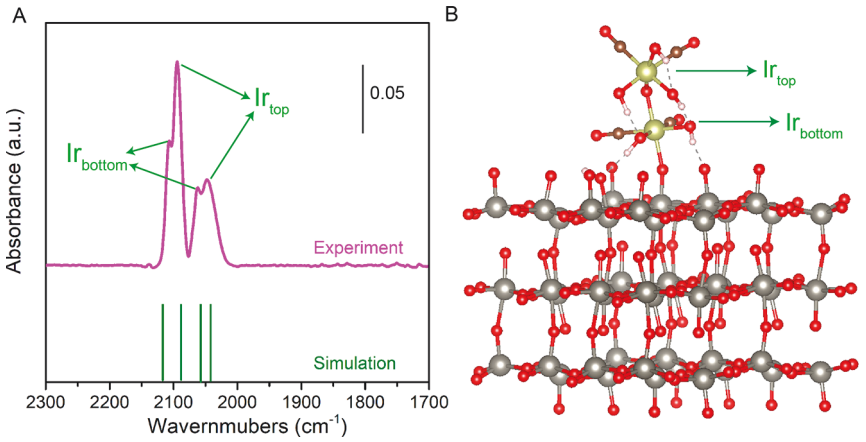


**Figure 2.** Determination of the binding mode of Ir DHCs on $WO_3$. (A) *In situ* CO DRIFTS spectra and the simulated peaks by DFT. (B) The structure model used for the simulation. Green ball: Ir, brown ball: C, red ball: O, white ball: H, and gray ball: W.

molecular catalysts for $CO_2$ and $H_2O$ reduction.[15,16] Chang et al. explored anchored supermolecular complexes for C−C coupling reactions by CO and $CO_2$ reduction.[17,18] This progress notwithstanding, the community sees a critical deficiency in this line of research in that there is a lack of direct experimental evidence to unambiguously support the proposed structures of the heterogenized catalysts. The deficiency has been partially addressed by Iwasawa et al.[19] and Gates et al., separately.[20−23] A breakthrough in studying the detailed structures of immobilized molecular catalysts was made recently by us on Ir dinuclear heterogeneous catalysts (DHCs), where unambiguous experimental data were obtained using high-angle annular dark-field scanning transmission electron microscopy (HAADF-STEM), extended X-ray absorption fine structure spectroscopy (EXAFS), and diffuse reflectance infrared Fourier transform spectroscopy (DRIFTS).[24]

While our latest result highlights the importance of the supporting substrate in facilitating the transformation of the molecular Ir homogeneous precursor to an Ir DHC, it raises an important question concerning the binding mode of the newly formed heterogeneous catalysts. That is, is the side-on binding mode as shown in Figure 1a the only way to stabilize the catalyst on a substrate? In other words, in the event where the supporting substrate lacks the binding pockets that would match the atomic distance between the two Ir centers, would we expect an end-on binding mode as shown in Figure 1b? Answers to this question are important not only because they hold the key to broad implementations of the synthesis strategy, but also because it has implications for the study of reaction mechanisms that would benefit from a second, dangling active metal center, similar to the $Mn_{dangling}$ center of the WOCs in natural photosystem II.[25] Here, we report a direct experimental observation of the end-on binding mode that provides a definitive answer to this question. The end-on bound Ir DHCs exhibit a higher activity toward water oxidation than the side-on bound Ir DHC or Ir single atom catalysts (SACs), possibly due to the flexibility of the top Ir center.

## SYNTHESIS STRATEGY FOR END-ON BOUND IRIDIUM DHCS

Our first task for this present work was to identify a supporting substrate that would favor the end-on binding mode. It was hypothesized that the side-on binding mode would be obtained



DOI: 10.1021/acscentsci.8b00335
ACS Cent. Sci. XXXX, XXX, XXX−XXX

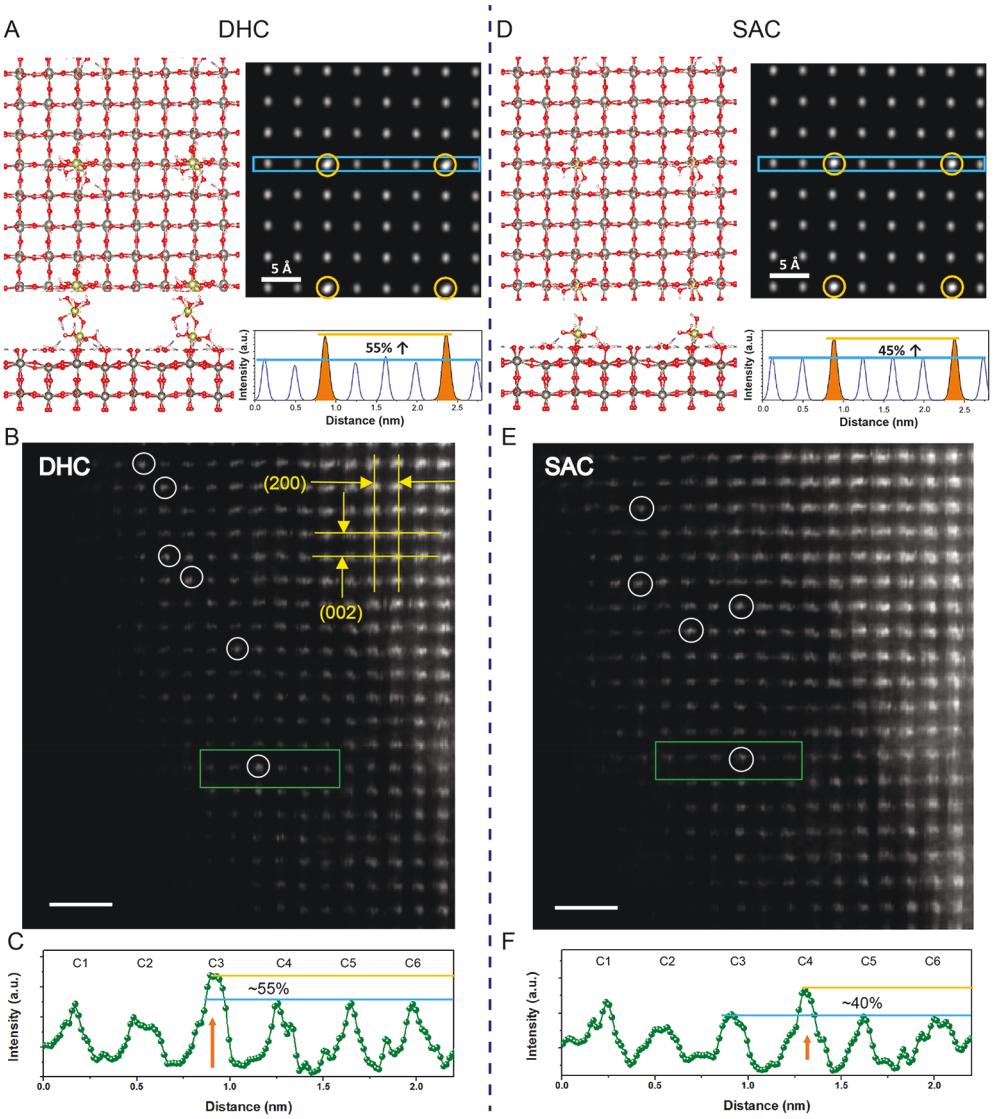


**Figure 3.** HAADF-STEM studies of end-on bound Ir DHCs on $WO_3$. (A) Atomic structure of Ir DHCs on top of $WO_3$ (020). Top left: top view; bottom left: side view. Simulated STEM image from the top view (top right), as well as a representative line scan profile of one Ir DHC against the $WO_3$ supporting substrate (bottom right). The positions of the Ir DHCs are marked by orange circles in the simulated STEM image, and the orange-shaded peaks indicate the position of Ir DHCs. (B) Experimental STEM image, in which the region for the line scan profile is marked by the green box. The white circles highlight Ir DHCs. (C) Line scan profile of the region highlighted in (B). (D) Simulated atomic structure of Ir SACs on top of $WO_3$ (020). The arrangement of the panels is identical to (A). (E) Experimental STEM image, in which Ir SACs are highlighted by the white circles. The green box marks the region where the line scan profile in (F) was obtained. (F) Line scan profile of the region shown in (E). Scale bars for (B) and (E): 1 nm.

when there are dual surface binding sites separated at or close to ca. 3.5 Å, which is the separation between two iridium atoms in the Ir molecular precursor. To test this hypothesis, we screened the following oxides, $Fe_2O_3$, $TiO_2$, $CeO_2$, and $WO_3$. It was found that, other than $WO_3$, all other oxides feature thermodynamically stable surfaces with a sufficiently high O density to construct two binding sites with suitable distances to stabilize a side-on bound Ir DHC (Figure S1 and Table S1 in Supporting Information). We, therefore, have chosen $WO_3$ as a study platform for this work. Building upon our recent successes in synthesizing Ir DHCs on $Fe_2O_3$, we carried out the synthesis by a soaking method, followed by UV treatments (see Supporting Information for experimental details). Subsequent X-ray photoelectron spectroscopy (XPS) and electron energy loss spectroscopy (EELS) studies confirmed that the N-containing pyalc ligands were completely removed (Figures S2 and S3 in Supporting Information).

## EVIDENCE OF THE BINDING MODE BY *IN SITU* DRIFTS

We next employed *in situ* DRIFTS to probe the Ir DHC structures. As has been shown by others and us, DRIFTS is a powerful technique to report on the relative positions of Ir atoms on a substrate.[24,26] Here our main goal was to distinguish the structure of the targeted end-on bound Ir DHCs from the following alternatives, (i) side-on bound Ir DHC, (ii) Ir SAC, and (iii) aggregated Ir nanoparticles. From the data shown in Figure 2a, we immediately ruled out the possibility that Ir nanoparticles were present, which would correspond to a broad peak at ca. 1850 $cm^{-1}$ due to the


DOI: 10.1021/acscentsci.8b00335
ACS Cent. Sci. XXXX, XXX, XXX−XXX

bridged CO adsorption between adjacent Ir atoms.[24] The second structure we ruled out was Ir SACs, which would yield two characteristic singlet peaks at 2096 and 2050 $cm^{-1}$ (Figure S4 in Supporting Information). Similarly, we excluded the possibility of side-on bound Ir DHCs by the lack of the dual singlet peaks in the DRIFTS (Figure S5 in Supporting Information). With all these alternative possibilities considered, the only natural conclusion supported by this set of data was that the unique dual doublet DRIFTS peaks centering at ca. 2100 and 2050 $cm^{-1}$ are due to the end-on bound Ir DHCs. Of these two groups of peaks, the doublet at the high wavenumber (ca. 2100 $cm^{-1}$) is ascribed to the asymmetric stretching of the CO probe, and that at the low wavenumber (ca. 2050 $cm^{-1}$) is due to the symmetric stretching. Within each doublet, the higher wavenumber peak (2110 and 2062 $cm^{-1}$) reports on the bottom Ir atom, and the lower wavenumber peak (2090 and 2044 $cm^{-1}$) reports on the top Ir atom.

Our understanding of the DRIFTS data is supported by density functional theory (DFT) calculations. For this purpose, we relaxed the Ir DHCs on $WO_3$ (020) surface terminated with O and $H_2O$ (Figure 2b, Table S2, and Figure S6). Here the $WO_3$ (020) surface was chosen because our X-ray diffraction (XRD) patterns and scanning transmission electron microscopy (STEM) data revealed that the $WO_3$ substrate studied in this project exhibited a preferable exposure of the (020) facets (Figure S7 in Supporting Information). The Ir−O−Ir unit is bound to $WO_3$ by a single O atom. Importantly, the structure model optimized by DFT permitted us to simulate the expected stretching frequencies of adsorbed CO on the end-on bound Ir DHCs. The calculated peak positions (2119, 2058 $cm^{-1}$ and 2087, 2043 $cm^{-1}$) are in excellent agreement with the experimental data, providing us strong confidence of the proposed structure as shown in Figure 2b.

## STRUCTURAL EVOLUTION FROM IR DHCS TO IRIDIUM SACS

Examinations of the structure as shown in Figure 2b prompted us to study how the structure of end-on bound Ir DHCs change under synthesis conditions. A critical concern we had to address was whether the end-on bound Ir DHCs would be readily transformed to Ir SACs by the breaking of the $\mu$-oxo bridge. It was found that under the preparation conditions (UVO cleaner system, more information in Supporting Information), we observed only Ir DHCs for durations at or shorter than 40 min. Interestingly, longer photochemical treatments (>40 min) only yielded aggregated Ir nanoparticles, but not Ir SACs. As a control experiment, we observed Ir SACs on $WO_3$ by *in situ* photochemical treatments in the DRIFTS apparatus or under e-beam irradiation in the STEM chamber (Figure S8 and associated *in situ* STEM discussions in Supporting Information). It is noted that the DRIFTS spectral features of Ir SAC on $WO_3$ are distinctly different from those of Ir DHCs, whereas the former exhibits two singlet peaks at 2096 and 2050 $cm^{-1}$ (Figure S4 in Supporting Information), in good agreement with the simulated data based on the DFT model of Ir SAC on $WO_3$. We were, therefore, encouraged to propose that $H_2O$ in the atmosphere during the photochemical treatments in the UVO cleaner chamber with the relatively high humidity facilitates Ir aggregation once an Ir DHC is decomposed. Preliminary DFT calculations show that the energy to break the $Ir_{top}$−O bond in the $Ir_{top}$−O−$Ir_{bottom}$ unit is comparable to that of the $Ir_{bottom}$−O bond in the $Ir_{bottom}$−O−W unit if the solvation effects of $H_2O$ are considered. The resulting stable structure would be Ir nanoparticles instead of Ir SAC. In the absence of $H_2O$ solvation effects, however, the $Ir_{bottom}$−O bond is stronger than the $Ir_{top}$−O one, suggesting that Ir SAC on $WO_3$ is favored once the Ir−O−Ir unit is dissociated (Figure S9 and more discussions in Supporting Information). When confirmed by further research, this understanding will likely have important implications for the efforts focused on the synthesis of atomically dispersed catalysts.

## FURTHER CONFIRMATION OF THE END-ON BINDING MODE BY HAADF-STEM

HAADF-STEM was subsequently carried out to directly visualize the end-on bound Ir DHCs on $WO_3$. While Ir DHCs may be readily distinguished from aggregated Ir nanoparticles by STEM, it is difficult to differentiate an end-on bound Ir DHC from an Ir SAC as both would appear in an STEM image as a single bright spot, due to the projective nature of STEM observations. The challenge is exacerbated by the fact that Ir and W feature comparable Z contrasts as a result of their close atomic weights. To combat this challenge, we simulated the HAADF-STEM data based on the structure model as shown in Figure 3a (left panel). For quantitative comparisons, the thickness of the simulated structure model (ca. 0.77 nm) was chosen to represent that of the observed sample, which was confirmed by the following complementary techniques for accuracy, low-loss EELS, STEM analysis and position averaged convergent beam electron diffraction (PACBED), as well as the associated simulations (Figures S10−12 in Supporting Information). We see from Figure 3a,d that the presence of an Ir DHC would yield an increase of the line scan intensity by 55%, whereas an Ir SAC would increase the intensity by 45%. Experimentally, we observed a ca. 55% increase in the Ir DHC (Figure 3c) and a ca. 40% increase in the Ir SAC (Figure 3f). Combining this set of data with the HAADF-STEM images (Figure 3b,e and Figure S13−14 in Supporting Information), as well as the DRIFTS data (Figure 2a), we concluded that we have successfully synthesized Ir DHCs in an end-on binding mode.

## CATALYTIC CHARACTERIZATION OF END-ON BOUND IR DHCS

With the structure and the binding mode of Ir DHCs on $WO_3$ confirmed, we next carried out $H_2O$ oxidation reactions to characterize the catalytic properties. For these experiments, we employed an electrolyte of pH 3.0 (0.1 M $K_2SO_4$, pH adjusted by $H_2SO_4$). Previous research has shown that $WO_3$ is active toward $H_2O$ oxidation, and the associated photocurrent−voltage ($J$−$V$) curves feature high fill factors (FF), indicative of fast charge transfer.[27] Such a characteristic was indeed observed by us. If we used the photocurrent density at 1.23 V vs RHE as the short-circuit current density ($J_{sc}$), and the voltage where 0.1 mA/$cm^2$ photocurrent was measured as the open-circuit potential[28] ($V_{oc}$) and treated the data as a diode-based solar cell, an FF of 0.37 would be obtained. By comparison, bare $Fe_2O_3$ would yield an FF of 0.19 without cocatalysts. The presence of Ir SACs and DHCs improved the FF marginally to 0.42 and 0.47, respectively (Figure S15). No measurable difference was observed between their turn-on characteristics.



DOI: 10.1021/acscentsci.8b00335
ACS Cent. Sci. XXXX, XXX, XXX−XXX

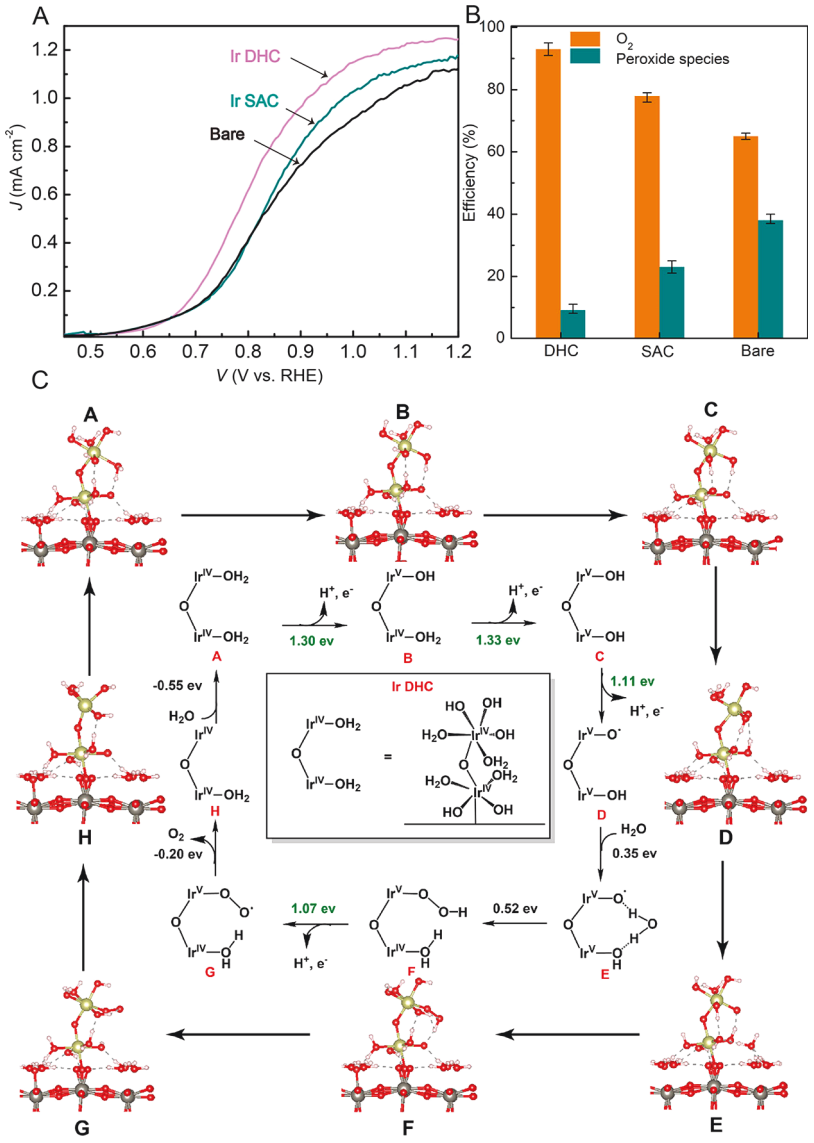


**Figure 4.** Catalytic activity of Ir DHC and SAC on $WO_3$, as well as bare $WO_3$. (A) Photocurrent density voltage data. (B) Product selectivity toward $O_2$ evolution vs peroxide species formation. The error bars represent variations of measurements on five different batches of samples. (C) Proposed mechanism of the Ir DHC as studied by DFT calculations. A–H in Figure 4C represent the DFT optimized intermediates.

The most critical difference between samples with and without Ir DHCs or SACs was found in the product selectivity. Due to slow kinetics toward a four-electon pathway to produce $O_2$, $WO_3$ is known to facilitate a two-electron pathway of $H_2O$ oxidation, yielding peroxides as a product.[29] By comparison, Ir-based catalysts are expected to favor the four-electron pathway of complete $H_2O$ oxidation to $O_2$.[30−33] We, therefore, performed product detections. As shown in Figure 4b, the total detected $O_2$ and peroxide account for ca. 100% of all charges measured. Among the samples studied, 38% of peroxides were measured on bare $WO_3$ under our experimental conditions; the number for Ir DHCs on $WO_3$ was only 9%, and that for Ir SACs on $WO_3$ was 23%. They strongly suggest that despite the catalytic activity of bare $WO_3$ toward two-electron $H_2O$ oxidation, charges prefer to find Ir catalytic sites for four-electron $H_2O$ oxidation. The competing process would be two-electron $H_2O$ oxidation on exposed $WO_3$ surfaces. The comparison between Ir DHCs and SACs further highlights the benefit of the second, dangling Ir atom in facilitating $H_2O$ oxidation reactions, the details of which were studied next by DFT.

The DFT calculations were conducted based on the proposed mechanism as shown in Figure 4c, where multiple proton-coupled electron transfer (PCET) steps are involved. Due to the coordination environment difference of the two Ir atoms in an end-on bound Ir DHC, $Ir_{top}$ was assumed to be slightly more electron rich. It would undergo PCET to build an oxidizing potential first (steps A → B in Figure 4c), followed by two consecutive PCET processes and the O-O bond formation step to yield Ir-OOH (F in Figure 4c). The free energy changes of the three PCET steps are 1.30, 1.33, and 1.11 eV, respectively, at $U$ = 0 V ($U$ is the applied potential; Figure 4c). When similar calculations were performed on Ir SACs on $WO_3$, it was found that a different pathway would be preferred (Figure S17 in Supporting Information) because a third PCET to oxidize the Ir SAC after the first two PCET steps would require too high an energy (1.85 eV; Figure S18 in Supporting Information). The results further highlight the benefit of having a second Ir site for four-electron $H_2O$


DOI: 10.1021/acscentsci.8b00335
ACS Cent. Sci. XXXX, XXX, XXX−XXX

oxidation. They set the stage for more accurate calculations to include potential influences by the supporting substrate ($WO_3$) and the solvents.

The DFT results of end-on bound Ir DHCs can also be compared with side-on bound Ir DHCs. As detailed in Figure S19, compared with the side-on bound Ir DHC, the end-on bound one consumed lower energy to bind water during the nucleophilic attack (D → E) and oxygen release (G → H) due to the flexibility of the Ir−O−Ir unit. Ideally, the comparison would be more meaningful if one could construct end-on and side-on bound Ir DHCs on the same substrate. Unfortunately, such a possibility is not yet observed experimentally. Our results show that when side-on binding is possible (owing to the relative closeness of Ir binding sites on the surface, such as on $Fe_2O_3$), no end-on bound Ir DHCs are observed. We, therefore, caution the qualitative nature of such a comparison as shown in Figures S19 and S20. Notwithstanding, the excellent performance of end-on bound Ir DHCs reminds us of the $Mn_{dangling}$ moiety in the $Mn_4CaO_5$ catalytic center in PSII, where it has been proposed that the dangling atom will lose electrons, and that $H_2O$ nucleophilic attack for the O−O bond formation may occur on the dangling Mn.[34] Within this context, we see that the results presented here may have significant implications for constructing catalysts with a similar structure flexibility for complex chemical reactions.

## CONCLUSIONS

The development of catalysis sees a clear trend of convergence, where the benefits of both molecular and heterogeneous catalysis may be combined for better overall performance in terms of TOFs and TONs. Within this context, we obtained an Ir DHC that maintains the atomic arrangement of the molecular precursor but is bound to the supporting substrate of $WO_3$ in an end-on mode. Spectroscopic (DRIFTS, EELS) and HAADF-STEM results strongly support the dinuclear nature of the catalyst, as well as the end-on binding mode. The binding mode is further supported by DFT calculations. Together with the previously reported side-on bound Ir DHCs, the results prove that rich configurations of atomically dispersed heterogeneous catalysts are possible. Importantly, the resulting catalysts show superior performance for $H_2O$ oxidation in comparison to bare substrate. As such, the results represent an important step toward tailor-designed, atomically defined heterogeneous catalysts for important chemical transformations such as solar fuel synthesis.

## ASSOCIATED CONTENT

### Supporting Information

The Supporting Information is available free of charge on the ACS Publications website at DOI: 10.1021/acscentsci.8b00335.

Details of synthesis, characterization, and computational methods (PDF)

## AUTHOR INFORMATION


### Corresponding Author

*E-mail: dunwei.wang@bc.edu.

### ORCID

Yanyan Zhao: 0000-0002-1428-5022
Xingxu Yan: 0000-0001-7991-4849
Qi Dong: 0000-0002-7553-4213
James E. Thorne: 0000-0002-7711-428X
Gary W. Brudvig: 0000-0002-7040-1892
Victor S. Batista: 0000-0002-3262-1237
Dunwei Wang: 0000-0001-5581-8799

### Author Contributions

#Y.Z., X.Y. and K.R.Y contributed equally.


### Notes

Safety Statement: No unexpected or unusually high safety hazards were encountered.

The authors declare no competing financial interest.

## ACKNOWLEDGMENTS

We thank Dr. Wenpei Gao and Mr. Christopher Addiego from UCI for position averaged convergent beam electron diffraction simulations. We thank Dr. Guanyu Liu for $WO_3$ sample preparation. We thank Dr. Stafford W. Sheehan, Dr. Wei Li, Mr. Da He, and Dr. Dongsheng Song for discussions. Work done at Boston College was in part supported by the National Science Foundation (CBET 1703663 and 1703655) for materials synthesis and photoelectrochemical studies; HAADF-STEM work at UCI was supported by DOE-BES (Grant No. DE-FG-05ER46237); X.Y. and X.P. acknowledge the support of the University of California, Irvine, Materials Research Institute for the use of TEM facilities; precursor synthesis and theoretical computations at Yale University were supported by the Argonne-Northwestern Solar Energy Research (ANSER) Center, an Energy Frontier Research Center funded by the U.S. Department of Energy (DOE), Office of Science, Office of Basic Energy Sciences, under Award Number DE-SC0001059; V.S.B and K.R.Y acknowledge the computer time from the national energy research scientific computing center (NERSC); *in situ* DRIFTS studies are supported by DE-FG02-05ER15730.

## REFERENCES


(1) Duan, L.; Bozoglian, F.; Mandal, S.; Stewart, B.; Privalov, T.; Llobet, A.; Sun, L. A Molecular Ruthenium Catalyst with Water-Oxidation Activity Comparable to That of Photosystem II. *Nat. Chem.* **2012**, *4*, 418.

(2) Flytzani-Stephanopoulos, M.; Gates, B. C. Atomically Dispersed Supported Metal Catalysts. *Annu. Rev. Chem. Biomol. Eng.* **2012**, *3*, 545.

(3) Yang, X.-F.; Wang, A.; Qiao, B.; Li, J.; Liu, J.; Zhang, T. Single-Atom Catalysts: A New Frontier in Heterogeneous Catalysis. *Acc. Chem. Res.* **2013**, *46*, 1740.

(4) Chen, Z.; Concepcion, J. J.; Jurss, J. W.; Meyer, T. J. Single-Site, Catalytic Water Oxidation on Oxide Surfaces. *J. Am. Chem. Soc.* **2009**, *131*, 15580.

(5) Alibabaei, L.; Brennaman, M. K.; Norris, M. R.; Kalanyan, B.; Song, W.; Losego, M. D.; Concepcion, J. J.; Binstead, R. A.; Parsons, G. N.; Meyer, T. J. Solar Water Splitting in a Molecular Photoelectrochemical Cell. *Proc. Natl. Acad. Sci. U. S. A.* **2013**, *110*, 20008.

(6) Vannucci, A. K.; Alibabaei, L.; Losego, M. D.; Concepcion, J. J.; Kalanyan, B.; Parsons, G. N.; Meyer, T. J. Crossing the Divide between Homogeneous and Heterogeneous Catalysis in Water Oxidation. *Proc. Natl. Acad. Sci. U. S. A.* **2013**, *110*, 20918.

(7) Li, F.; Fan, K.; Wang, L.; Daniel, Q.; Duan, L.; Sun, L. Immobilizing Ru(bda) Catalyst on a Photoanode via Electrochemical Polymerization for Light-Driven Water Splitting. *ACS Catal.* **2015**, *5*, 3786.

(8) Wang, Y.; Li, F.; Zhou, X.; Yu, F.; Du, J.; Bai, L.; Sun, L. Highly Efficient Photoelectrochemical Water Splitting with an Immobilized




DOI: 10.1021/acscentsci.8b00335
ACS Cent. Sci. XXXX, XXX, XXX−XXX

Molecular $Co_4O_4$ Cubane Catalyst. *Angew. Chem., Int. Ed.* **2017**, *56*, 6911.
(9) Sheehan, S. W.; Thomsen, J. M.; Hintermair, U.; Crabtree, R. H.; Brudvig, G. W.; Schmuttenmaer, C. A. A Molecular Catalyst for Water Oxidation That Binds to Metal Oxide Surfaces. *Nat. Commun.* **2015**, *6*, 6469.
(10) Yang, K. R.; Matula, A. J.; Kwon, G.; Hong, J.; Sheehan, S. W.; Thomsen, J. M.; Brudvig, G. W.; Crabtree, R. H.; Tiede, D. M.; Chen, L. X.; Batista, V. S. Solution Structures of Highly Active Molecular Ir Water-Oxidation Catalysts from Density Functional Theory Combined with High-Energy X-Ray Scattering and EXAFS Spectroscopy. *J. Am. Chem. Soc.* **2016**, *138*, 5511.
(11) Ahn, H. S.; Yano, J.; Tilley, T. D. Photocatalytic Water Oxidation by Very Small Cobalt Domains on a Silica Surface. *Energy Environ. Sci.* **2013**, *6*, 3080.
(12) Rumberger, E. M. W.; Ahn, H. S.; Bell, A. T.; Tilley, T. D. Water Oxidation Catalysis via Immobilization of the Dimanganese Complex $[Mn_2(\mu\text{-}O)_2Cl(\mu\text{-}O_2CCH_3)\text{-}(bpy)_2(H_2O)](NO_3)_2$ onto Silica. *Dalton Trans.* **2013**, *42*, 12238.
(13) Ye, S.; Ding, C.; Chen, R.; Fan, F.; Fu, P.; Yin, H.; Wang, X.; Wang, Z.; Du, P.; Li, C. Mimicking the Key Functions of Photosystem II in Artificial Photosynthesis for Photoelectrocatalytic Water Splitting. *J. Am. Chem. Soc.* **2018**, *140*, 3250.
(14) Ye, S.; Chen, R.; Xu, Y.; Fan, F.; Du, P.; Zhang, F.; Zong, X.; Chen, T.; Qi, Y.; Chen, P.; Chen, Z.; Li, C. An Artificial Photosynthetic System Containing an Inorganic Semiconductor and a Molecular Catalyst for Photocatalytic Water Oxidation. *J. Catal.* **2016**, *338*, 168.
(15) Warnan, J.; Willkomm, J.; Ng, J. N.; Godin, R.; Prantl, S.; Durrant, J. R.; Reisner, E. Solar $H_2$ Evolution in Water with Modified Diketopyrrolopyrrole Dyes Immobilised on Molecular Co and Ni Catalyst-$TiO_2$ Hybrids. *Chem. Sci.* **2017**, *8*, 3070.
(16) Rosser, E. T.; Windle, D. C.; Reisner, E. Electrocatalytic and Solar-Driven $CO_2$ Reduction to CO with a Molecular Manganese Catalyst Immobilized on Mesoporous $TiO_2$. *Angew. Chem., Int. Ed.* **2016**, *55*, 7388.
(17) Gong, M.; Cao, Z.; Liu, W.; Nichols, E. M.; Smith, P. T.; Derrick, J. S.; Liu, Y.-S.; Liu, J.; Wen, X.; Chang, C. J. Supramolecular Porphyrin Cages Assembled at Molecular-Materials Interfaces for Electrocatalytic CO Reduction. *ACS Cent. Sci.* **2017**, *3*, 1032.
(18) Cao, Z.; Derrick, J. S.; Xu, J.; Gao, R.; Gong, M.; Nichols, E. M.; Smith, P. T.; Liu, X.; Wen, X.; Copéret, C.; Chang, C. J. Chelating N-Heterocyclic Carbene Ligands Enable Tuning of Electrocatalytic $CO_2$ Reduction to Formate and Carbon Monoxide: Surface Organometallic Chemistry. *Angew. Chem., Int. Ed.* **2018**, *57*, 4981.
(19) Ichikuni, N.; Iwasawa, Y. Structures and Catalysis of New Nb Dimers on $SiO_2$. *Catal. Today* **1993**, *16*, 427.
(20) Han, C. W.; Iddir, H.; Uzun, A.; Curtiss, L. A.; Browning, N. D.; Gates, B. C.; Ortalan, V. Migration of Single Iridium Atoms and Tri-Iridium Clusters on MgO Surfaces: Aberration-Corrected Stem Imaging and Ab Initio Calculations. *J. Phys. Chem. Lett.* **2015**, *6*, 4675.
(21) Lu, J.; Serna, P.; Aydin, C.; Browning, N. D.; Gates, B. C. Supported Molecular Iridium Catalysts: Resolving Effects of Metal Nuclearity and Supports as Ligands. *J. Am. Chem. Soc.* **2011**, *133*, 16186.
(22) Yang, D.; Xu, P.; Browning, N. D.; Gates, B. C. Tracking Rh Atoms in Zeolite Hy: First Steps of Metal Cluster Formation and Influence of Metal Nuclearity on Catalysis of Ethylene Hydrogenation and Ethylene Dimerization. *J. Phys. Chem. Lett.* **2016**, *7*, 2537.
(23) Yang, D.; Xu, P.; Guan, E.; Browning, N. D.; Gates, B. C. Rhodium Pair-Sites on Magnesium Oxide: Synthesis, Characterization, and Catalysis of Ethylene Hydrogenation. *J. Catal.* **2016**, *338*, 12.
(24) Zhao, Y.; Yang, K. R.; Wang, Z.; Yan, X.; Cao, S.; Ye, Y.; Dong, Q.; Zhang, X.; Thorne, J. E.; Jin, L.; Materna, K. L.; Trimpalis, A.; Bai, H.; Fakra, S. C.; Zhong, X.; Wang, P.; Pan, X.; Guo, J.; Flytzani-Stephanopoulos, M.; Brudvig, G. W.; Batista, V. S.; Wang, D. Stable Iridium Dinuclear Heterogeneous Catalysts Supported on Metal-Oxide Substrate for Solar Water Oxidation. *Proc. Natl. Acad. Sci. U. S. A.* **2018**, *115*, 2902.
(25) Vinyard, D. J.; Brudvig, G. W. Progress toward a Molecular Mechanism of Water Oxidation in Photosystem II. *Annu. Rev. Phys. Chem.* **2017**, *68*, 101.
(26) Hoffman, A. S.; Debefve, L. M.; Zhang, S.; Perez-Aguilar, J. E.; Conley, E. T.; Justl, K. R.; Arslan, I.; Dixon, D. A.; Gates, B. C. Beating Heterogeneity of Single-Site Catalysts: MgO-Supported Iridium Complexes. *ACS Catal.* **2018**, *8*, 3489.
(27) Liu, R.; Lin, Y.; Chou, L.; Sheehan, S. W.; He, W.; Zhang, F.; Hou, H. J. M.; Wang, D. Water Splitting by Tungsten Oxide Prepared by Atomic Layer Deposition and Decorated with an Oxygen-Evolving Catalyst. *Angew. Chem., Int. Ed.* **2011**, *50*, 499.
(28) The current and voltage choices are just for qualitative comparison purposes.
(29) Klepser, B. M.; Bartlett, B. M. Anchoring a Molecular Iron Catalyst to Solar-Responsive $WO_3$ Improves the Rate and Selectivity of Photoelectrochemical Water Oxidation. *J. Am. Chem. Soc.* **2014**, *136*, 1694.
(30) Hintermair, U.; Sheehan, S. W.; Parent, A. R.; Ess, D. H.; Richens, D. T.; Vaccaro, P. H.; Brudvig, G. W.; Crabtree, R. H. Precursor Transformation During Molecular Oxidation Catalysis with Organometallic Iridium Complexes. *J. Am. Chem. Soc.* **2013**, *135*, 10837.
(31) Li, W.; He, D.; Sheehan, S. W.; He, Y.; Thorne, J. E.; Yao, X.; Brudvig, G. W.; Wang, D. Comparison of Heterogenized Molecular and Heterogeneous Oxide Catalysts for Photoelectrochemical Water Oxidation. *Energy Environ. Sci.* **2016**, *9*, 1794.
(32) Li, W.; Sheehan, S. W.; He, D.; He, Y.; Yao, X.; Grimm, R. L.; Brudvig, G. W.; Wang, D. Hematite-based Solar Water Splitting in Acidic Solutions: Functionalization by Mono- and Multilayers of Iridium Oxygen-Evolution Catalysts. *Angew. Chem., Int. Ed.* **2015**, *54*, 11428.
(33) Thomsen, J. M.; Sheehan, S. W.; Hashmi, S. M.; Campos, J.; Hintermair, U.; Crabtree, R. H.; Brudvig, G. W. Electrochemical Activation of Cp* Iridium Complexes for Electrode-Driven Water-Oxidation Catalysis. *J. Am. Chem. Soc.* **2014**, *136*, 13826.
(34) Barber, J. A Mechanism for Water Splitting and Oxygen Production in Photosynthesis. *Nat. Plants* **2017**, *3*, 17041.


DOI: 10.1021/acscentsci.8b00335
*ACS Cent. Sci.* XXXX, XXX, XXX−XXX